



Published in final edited form as:

*J Mater Sci Mater Med.* 2013 October ; 24(10): . doi:10.1007/s10856-013-4999-x.

## Matrix generation within a macroporous non-degradable implant for osteochondral defects is not enhanced with partial enzymatic digestion of the surrounding tissue: evaluation in an in vivo rabbit model

Aaron J. Krych, Florian Wanivenhaus, Kenneth W. Ng, Stephen Doty, Russell F. Warren, and Suzanne A. Maher

Hospital for Special Surgery, 535 East 70th Street, New York, NY 10021, USA

Suzanne A. Maher: mahers@hss.edu

### Abstract

Articular cartilage defects are a significant source of pain, have limited ability to heal, and can lead to the development of osteoarthritis. However, a surgical solution is not available. To tackle this clinical problem, non-degradable implants capable of carrying mechanical load immediately after implantation and for the duration of implantation, while integrating with the host tissue, may be viable option. But integration between articular cartilage and non-degradable implants is not well studied. Our objective was to assess the in vivo performance of a novel macroporous, nondegradable, polyvinyl alcohol construct. We hypothesized that matrix generation within the implant would be enhanced with partial digestion of the edges of articular cartilage. Our hypothesis was tested by randomizing an osteochondral defect created in the trochlea of 14 New Zealand white rabbits to treatment with: (i) collagenase or (ii) saline, prior to insertion of the implant. At 1 and 3-month post-operatively, the gross morphology and histologic appearance of the implants and the surrounding tissue were assessed. At 3 months, the mechanical properties of the implant were also quantified. Overall, the hydrogel implants performed favorably; at all time-points and in all groups the implants remained well fixed, did not cause inflammation or synovitis, and did not cause extensive damage to the opposing articular cartilage. Regardless of treatment with saline or collagenase, at 1 month post-operatively implants from both groups had a contiguous interface with adjacent cartilage and were populated with chondrocyte-like cells. At 3 months fibrous encapsulation of all implants was evident, there was no difference between area of aggrecan staining in the collagenase versus saline groups, and implant modulus was similar in both groups; leading us to reject our hypothesis. In summary, a porous PVA osteochondral implant remained well fixed in a short term in vivo osteochondral defect model; however, matrix generation within the implant was not enhanced with partial digestion of adjacent articular cartilage.

### 1 Introduction

Articular cartilage defects are a significant source of pain, have a limited ability to heal, and can lead to the development of osteoarthritis [1, 2]. Surgical options for symptomatic cartilage defects include palliative, reparative, and restorative methods [3], with the treatment algorithm and surgical indications for each procedure continuing to evolve [4, 5]. More recently, implants intended to encourage the formation of articular cartilage in the

defect site have been developed, many of which are biodegradable with mechanical properties that are continually changing, and often inferior to that of the native tissue during the degradation process [6]. Furthermore, the implants rely on a controlled and robust cellular response in order to recreate an organized tissue that looks and mechanically functions like the native articular cartilage; a goal that has thus far proven elusive in the biological environment of the defective knee. To tackle this clinical problem, well characterized, non-degradable implants capable of carrying mechanical load immediately after implantation and for the duration of implantation, while integrating with the host tissue, may be viable option. However few non-degradable implants for the treatment of osteochondral or chondral defects have transitioned to clinical use. This is in part because of the challenges in meeting the functional requirements in the mechanically demanding environment of the knee joint. For example, non-degradable constructs should ideally act as implants that can integrate with adjacent tissue, transfer load to the underlying bone (to avoid bony resorption), resist wear, and not cause abrasion to opposing cartilage surfaces.

Poly(vinyl alcohol) (PVA) is a hydrophilic non-degradable hydrogel, the mechanical properties of which can be readily controlled to provide the necessary mechanical support for the use in diarthrodial joints [6, 7]. Several studies have evaluated solid, non-porous PVA as a candidate material for chondral or osteochondral defects in animal models; but integration of the implant with adjacent articular cartilage was absent [7, 8], threatening the long-term functional ability of the implants. To tackle the challenge of integration, we recently developed a macro-porous PVA implant intended to allow cells from the host tissue to migrate into the implant. The macroporous scaffolds were manufactured by infiltrating PVA solutions at concentrations of up to 20 % wt/vol through surgical gelatin sponges. After a series of freeze–thaw cycles, and digestion of the sponge, an interconnected porous scaffold that chondrocytes could infiltrate was produced [9]. By varying the geometry of the gelatin sponge, the porosity of the scaffold (volume of pores, pore diameter, and pore distribution) can be controlled; furthermore, the mechanical properties of the scaffold (specifically, modulus) can be varied as a function of percent PVA content [9]. Using an in vitro model, we demonstrated that chondrocytes from surrounding articular cartilage could migrate into the porous PVA scaffolds, and that chondrocyte infiltration was increased by pre-treating the cartilage with collagenase prior to implant insertion [10]. However, the in vivo behavior of the implant has not thus far been explored.

The objective of this study was to assess the performance of a novel macroporous, nondegradable polyvinyl alcohol implant in an in vivo osteochondral defect model. We hypothesized that matrix generation within the implant would be enhanced with partial digestion of the edges of articular cartilage. Our hypothesis was tested by creating an osteochondral trochlear defect in a New Zealand white rabbit; randomizing the defect to (i) treatment with collagenase or (ii) treatment with saline, prior to insertion of the PVA macroporous implant; and assessing morphology and histologic appearance of the implant and adjacent tissue, and mechanical properties of the implant at 1 and 3-month post-operatively.

## 2 Methods

### 2.1 Implant fabrication

Surgical gelatin sponges (Ethicon-Johnson & Johnson, Somerville, NJ, USA) were saturated with deionized water and then soaked in a graded series of PVA solutions (Sigma-Aldrich, Saint Louis, MO, USA) to a final solution of 10 % w/v PVA [9]. The implants were subjected to 6 freeze–thaw cycles (–20 °C 20 h, 25 °C 4 h), digested in 500 U/mL of collagenase at 37 °C for 14 h, and cored to result in 5 mm × 4 mm implants. The implants were washed in 70 and 100 % ethanol solutions for 20 min each and then completely dried

in a laminar flow hood resulting in a non-degradable porous implant that was 80 % porous, with average pore sizes of 16  $\mu\text{m}$  (range 8–304  $\mu\text{m}$ ) [9].

## 2.2 Study design

The sample size for our in vivo study was calculated based on a power analysis of the number of cells that migrated into the implant as a function of pre-treatment with collagenase in an in vitro model [11]. Five knees were required for each group at each timepoint to obtain a power of 0.80 with  $\alpha = 0.05$ . With a bilateral model and two time-points for sacrifice (1 and 3 months) this resulted in a total of 10 rabbits. To account for unexpected animal loss, an additional rabbit was included in the study. Finally, three additional rabbits were included at the 3 months timepoint so that the mechanical properties of the site of implantation could be assessed. Thus, 14 adult male New Zealand white rabbits weighing 2.5–3.0 kg were obtained from Covance (Princeton, NJ, USA), and were operated on bilaterally; 6 of which were euthanized at 1 month and 8 of which were euthanized at 3-month post-operatively. The study was approved by our Institutional Animal Care and Use Committee.

## 2.3 Surgical implantation

All rabbits were preanesthetized by subcutaneous injection of 35 mg/kg ketamine and 5 mg/kg xylazine. Preoperative analgesia with 0.05 mg/kg buprenorphine was administered, along with 250 mg intramuscular ampicillin. Before surgery, rabbits were shaved and general anesthesia was induced by isoflurane. A medial parapatellar arthrotomy of the knee joint was performed. The patella was laterally subluxed to expose the trochlea. A constant point in the central articulating groove of the distal trochlea was localized, and a 3.5 mm cannulated drill over a guide wire was used to create an osteochondral defect 4 mm deep. The cartilage edges were incised sharply with a 3.5 mm biopsy punch to remove any ragged articular cartilage margins. The right/left knees were then randomized to the following groups (i) 15 min treatment with collagenase type II (10 U/mL, Worthington Biochemicals, Lakewood, NJ, USA) followed by saline irrigation, and (ii) treatment with normal saline for 15 min. For both groups, the solution (collagenase or saline) was placed in a syringe and injected into the defect until the solution filled the site to a level contiguous with the top surface of the adjacent articular cartilage. The cartilage surface was then covered with surgical sterile gauze; and the knee was manually secured to avoid unintended movements. After 15 min, the gauze was removed, the solution was extracted with a syringe and the defect site was irrigated with saline. The defect was then dried with gauze, and the 5 mm implant was press-fit into the defect. Within minutes the implant rehydrated with blood to create a stable, press-fit construct (Note: The effect of press-fit was determined from our previous in vitro work, which determined that a 5 mm implant in a 3.5 mm defect resulted in optimal interfacial strength and increased GAG content within the implant as a function of time [10]). The patella was reduced, and the knee was placed through a range of motion to ensure stability of the plug. The arthrotomy and skin was closed in layers with suture. The rabbits were returned to their cages, not immobilized, and allowed activity as tolerated. Six rabbits were euthanized at 1 month, and eight rabbits were euthanized at 3 months.

## 2.4 Gross inspection

The knees were exposed through the same medial para-patellar arthrotomy, and the knee joint, including the patella, was harvested en bloc. Gross examinations were performed to assess for implant loosening or synovitis. The International Cartilage Repair System (ICRS) Macroscopic Evaluation of Cartilage Repair was used to assess the gross appearance of the implants and surrounding articular cartilage under loupes 3 $\times$  magnification. Briefly, the ICRS describes: (1) the defect repair (grade 0 no fill, grade 4 flush to surrounding cartilage);

(2) integration to border zone (grade 0 no integration, grade 4 complete integration); and (3) macroscopic appearance (grade 0 total degeneration of graft, grade 4 intact smooth surface). The overall repair assessment is the summation of the three scores and rated as follows: grade I: normal (12); grade II: nearly normal (8–11); grade III: abnormal (4–7), grade IV severely abnormal (1–3) [11, 12].

One knee from the 1 month group and one knee from the 3 months group were randomly chosen for imaging using an environmental scanning electron microscope (Quanta 600; FEI Company, Hillsboro, OR) at 10 kV.

## 2.5 Histology

Knees for histological analysis had the patellofemoral articulation isolated from each joint and were placed in 10 % formalin with 1 % cetyl pyridinium chloride. The knees were then decalcified in 10 % EDTA in 0.05 M tris buffer (pH 7.4), which was changed every 3–4 days. The decalcified knees were embedded in paraffin and longitudinally sectioned into 8  $\mu\text{m}$ -thick slices. Slices were stained with Alcian Blue and Safranin-O to assess the articular cartilage morphology. Immunostains for localization of chondroitin sulfate, types I and II collagen, and aggrecan were also performed. Stained sections were microscopically examined for the relationship between the implant and the articular cartilage surface (flush, recessed, or proud), damage to adjacent articular cartilage margins, presence of tissue integration or fibrous encapsulation at both the articular cartilage and bony margins, and the presence of cells with chondrocyte morphology (chondrocyte-like) within the implant. A grading system based on the O'Driscoll method [13] was used to grade the articular cartilage surrounding the implant. The grading system was as follows: grade 4 = normal cellularity, no clusters, normal staining; grade 3 = normal cellularity, mild clusters, moderate staining; grade 2 = mild or moderate hypocellularity, slight staining; grade 1 = severe hypocellularity, poor or no staining; grade 0 = severe disruption, including fibrillation. Two slides from each knee were graded by two independent observers.

## 2.6 Aggrecan staining quantification

The area of aggrecan staining, adjusted for the porosity of the implant and expressed as a percent of total implant area, was calculated. Briefly, Bioquant Osteo II software (V8.10.20, Bioquant image analysis corporation, Nashville, TN) was used to manually select the aggrecan threshold range of staining in the native adjacent cartilage; the implant was selected as the region of interest; and the percent of the aggrecan positive stain highlighted at the chosen threshold was calculated. This was repeated six times for each implant, by two blinded observers. Inter-rater reliability showed excellent agreement, with an intra-class correlation coefficient of 0.91 (95 % confidence interval 0.61–0.99).

## 2.7 Mechanical testing protocol

Experimental knees for mechanical testing ( $n = 3$  per group at 3 months) were frozen immediately after harvest; thereafter thawed 24 h prior to testing, at which point they were individually placed on the base of an Enduratec ELF materials testing machine (Bose, Minnetonka, MN), oriented so that the implant was perpendicular to the indentation fixture, and clamped in place. A porous indenter (diameter 1.25 mm) was attached to the upper actuator. A pre-designed program was used to apply a compressive load of 20 g at a rate of 5 g/s; thereafter the load was kept constant for 1 h. At the completion of testing the indentation fixture was replaced with a needle fixture to measure implant thickness. Displacement–time data were numerically fit to the biphasic indentation creep solution to determine three intrinsic material coefficients at each test site: aggregate modulus (Ha) and permeability (k) as described previously [14]. Values for the shear modulus ( $\mu$ ) were calculated from the parameters, Ha and  $\mu$ . The data generated was compared to that from four cadaveric rabbit

knees in which an identical defect and an identical implant was placed (time zero mechanical properties).

## 2.8 Statistical analysis

Cartilage grading (ICRS and modified O'Driscoll scoring system), area of aggrecan staining, and mechanical test data (Ha,  $\mu$  k) were analyzed using two-way ANOVA with time and treatment as independent variables. Bonferroni post hoc analysis was performed with an  $\alpha = 0.05$  to determine significance. Statistical analysis was performed using GraphPad Prism v4.0 software (GraphPad Software, Inc.; La Jolla CA).

## 3 Results

### 3.1 Gross inspection

At 1 month, there was no evidence of synovitis and the implants had a stable interface with adjacent articular cartilage. All specimens in both groups had an ICRS score of 12 indicating an intact implant smooth surface that was flush to the surrounding cartilage, complete integration with surrounding cartilage, and an intact smooth surface. Similarly, at 3 months, the eight knees in the collagenase-treated group (five knees for histology and three for mechanical testing) and the eight knees in the control group had no evidence of synovitis, the implant interface with adjacent articular cartilage appeared to be continuous without gross evidence of gaps, and all specimens had an ICRS score of 12. Environmental scanning electron microscopy at 1 month correlated well with gross observations demonstrating good integration between the implant and surrounding articular cartilage and bone (Fig. 1a). However, at the 3 months time point, fibrous encapsulation of the implant was apparent (Fig. 1b).

As illustrated in Table 1, gross inspection of the patellas revealed ICRS scores of between 10 and 12 at both one and 3 months. Specifically, at 1 month in the collagenase-treated group the scores were as follows: score of 10 in three knees, score of 11 in two knees and score of 12 in one knee. At 3 months, one knee had a score of 10, one knee had a score of 11 and three had a score of 12. In the saline group scores were as follows:  $n = 3$ , score of 10,  $n = 2$  score of 11 and  $n = 1$  score of 12 at 1 month;  $n = 1$  score of 10,  $n = 3$  score of 11 and  $n = 1$  score of 12 at 3 months. There was no statistically significant difference between ICRS scores of the patella as a function of time or treatment.

### 3.2 Histological analysis

At 1 month, PVA implants were populated with chondrocyte-like cells, many of which were producing type II collagen, chondroitin sulfate, and aggrecan. The implants in both the collagenase-treated and control groups were flush with the articular surface and adjacent articular cartilage was free from any discernable damage (Fig. 2a). Shrinkage of implants occurred due to water loss during histological processing; a factor which complicated the assessment of the implant-cartilage interface. Nonetheless, in all cases, the profile of the shrunken implant matched that of the adjacent cartilage walls, suggesting that an intimate interface had existed prior to processing (Fig. 2b). At the bone-implant interface, 50 % in each group had some evidence of tissue integration (Fig. 2c), while all had some fibrous tissue present at this interface. All implants in both treatment groups had cells with chondrocyte-like morphology within the implant (Fig. 2d).

There was no significant difference in the modified O'Driscoll scoring system as a function of time or treatment. In the collagenase group at 1 month, two knees had a score of four and four knees had a score of three; while in the saline treated group, one knee had a score of 4 and five knees had a score of three. At 3-month post-operatively, in the collagenase-treated

group one knee had a score of four, three had a score of three, and one knee had a score of two. In the saline treated group, one knee had a score of four and all remaining three knees had a score of three.

At 3 months, fibrous encapsulation of the PVA implants was present at both the articular cartilage and bony interfaces, but there was no evidence of macrophages or giant cells. Three of five implants (60 %) in the collagenase-treated group were slightly recessed with the remaining two flush. In the control group, two of the five implants were slightly recessed with the remaining three implants flush; adjacent articular cartilage was not damaged. All of the implants in both groups had presence of fibrous tissue at the adjacent articular cartilage interface (Fig. 3a) as well as at the bone-implant interface (Fig. 3b). Two of five implants in the collagenase-treated group (40 %) and three of five (60 %) implants in the control group had some chondrocyte-like cells remaining within the implant and staining for type II collagen, chondroitin sulfate, and aggrecan was largely present in all slides. The histological findings are summarized in Table 2.

### 3.3 Aggrecan staining quantification

There was no significant difference between area of aggrecan in the collagenase versus saline treated defects at 1 (16.6 vs. 12.5 %) or 3 months (14.5 vs. 10.7 %; Table 3).

### 3.4 Mechanical testing protocol

There was no significant difference as a function of time (time zero vs. 3 months) and as a function of treatment (saline vs. collagenase) in Ha,  $\mu$ , and k. At 3-month postoperatively, Ha values ranged from 0.2 to 1.5 MPa for the collagenase-treated group and 0.4–1.0 MPa in the saline treated group;  $\mu$  ranged from 0.1 to 0.6 MPa for the collagenase group and 0.22–0.35 MPa for the saline treated group; k ranged from 0.29–7.58  $\times 10^{-15}$  m<sup>4</sup>/Ns in the collagenase group and 0.22–3.09  $\times 10^{-15}$  m<sup>4</sup>/Ns in the saline treated group. The time zero data was as follows: Ha: 0.3–1.7 MPa;  $\mu$ : 0.12–0.74 MPa and k: 0.54–5.94  $\times 10^{-15}$  m<sup>4</sup>/Ns.

## 4 Discussion

The objective of this study was to assess the performance of a novel macroporous, nondegradable polyvinyl alcohol implant in an in vivo osteochondral defect model. Our hypothesis, that matrix generation within the implant would be enhanced with partial digestion of the edges of articular cartilage, was tested by randomizing an osteochondral trochlear defect in a New Zealand white rabbit to: (i) treatment with collagenase or (ii) treatment with saline, prior to insertion of the implant. At 1 and 3-month postoperatively, the gross morphology and histologic appearance of the implants and the surrounding tissue were assessed. At 3 months, the mechanical properties of the implant were also quantified. The implants remained fixed in the defect site at all time-points; they integrated with surrounding tissue, did not cause inflammation or synovitis, and did not cause extensive damage to the opposing articular cartilage. Mild degeneration of the adjacent articular cartilage was seen in the form of localized clustering of a small number of chondrocytes and moderate staining at time-points of up to 3 months. It is difficult to know if these findings were the result of the presence of an implant, or if they would have occurred if the defect had been left empty. Fibrous tissue encapsulation of the implant was evident in all knees at 3 months. Finally, as a quantitative measure of cellular migration into the implant and matrix production within the implant, area of aggrecan staining was similar in the collagenase and saline treated groups at both time-points. Therefore, our hypothesis that in vivo migration into the implant would be superior with predigestion of adjacent cartilage with collagenase was rejected.

The concept of using a non-degradable implant for the treatment of focal cartilage defects is not new [15, 16] and the avoidance of requiring host cells to re-create functional native



tissue is a clear advantage to such implants. Ideally, a non-degradable implant for focal osteochondral defects should have an ability to integrate with surrounding tissue, biomechanically distribute load to the underlying bone, and protect adjacent cartilage from further degradation [8]. However, integration between implants and the adjacent articular cartilage has been problematic. We previously developed a porous PVA implant to address this problem, and demonstrated its ability to allow for chondrocyte migration, matrix generation and increased interfacial strength with articular cartilage *in vitro*; which was enhanced with the application of collagenase to the host articular cartilage prior to scaffold implantation; [10] but the *in vivo* response has thus far not been assessed.

The concept of partially digesting the edges of articular cartilage in order to free chondrocytes from their dense matrix so that they can migrate has been explored by other using *in vivo* models. Lee et al. [17] demonstrated increased adhesive force of chondrocytes to articular cartilage in response to chondroitinase digestion and van de Breevaart Bravenboer et al. [18] showed improved cartilage–cartilage integration after using hyaluronidase and collagenase treatment. In a rabbit model Hunziker et al. [19] observed a greater extent of repair cells at the site of a superficial chondral lesion treated with chondroitinase when compared to control [19]. However, the effect of digestion on articular cartilage integration with an implant has not previously been explored. In contrast to our *in vitro* study which also used a digestion time of 15 min [10], collagenase pre-digestion of the surrounding cartilage did not improve cellular migration *in vivo*; the main difference between which was the use of a chondral model *in vitro*, and an osteochondral model *in vivo*. Articular cartilage in the rabbit is approximately 600  $\mu\text{m}$  thick [20], which does not allow for a sufficiently robust implant-cartilage interface using our implant press-fit approach, thus we thus decided to use an osteochondral defect to provide additional fixation to the implant.

The most prevalent histologic change over time was the presence of progressive fibrous encapsulation, especially at the implant-bone interface, which occurred in all 10 animal knees at 3 months. The lack of integration may have been caused in part by a foreign body response combined with an inability of osteoblasts to migrate into and remain in the porous morphology of the scaffold. The principal requirements for osseointegration include biomaterial biocompatibility, appropriate pore size, small implant-bone interface distances, and minimal implant micromotion [21]. Multiple studies have shown that the optimal pore size range to allow for osseointegration is 100–400  $\mu\text{m}$ , and almost all porous-coated prostheses available for clinical use in the area of joint replacement have pore sizes in this range [22]. The average pore size for the porous PVA implant in this study was 16  $\mu\text{m}$  (range 8–304  $\mu\text{m}$ ) [9], which although suitable for chondrocyte migration [10] may not be large enough to allow for bony ingrowth. The mis-match in modulus between the PVA implant and bone and the resulting micro motion of the implant, was also a likely contributing factor to the development of the fibrous membrane [23]. One potential solution to improve integration with bone would be to fabricate a bilayered implant; the porosity and stiffness of each layer can then be manipulated to determine the tissue types that grow within it [24, 25], a concept which has been used in the design of many implants that are currently undergoing clinical evaluation [26–29].

The current study has several limitations. The first is that breaching the subchondral bone likely created an environment of a mixed cellular population within the implant, similar to microfracture [30] in contrast to our preliminary *in vitro* work. Secondly, a negative control (unfilled defect) was not used in this study because its inclusion would not have helped us to test our hypothesis. Nonetheless, its exclusion hampered our ability to truly identify the cause of the mild degenerative changes seen in the adjacent articular cartilage. Thirdly, while no implant became dislodged from the defect site, the long-term consequences of the

fibrous encapsulation may have led to loosening in a longer-term animal model. Finally, a cannulated drill to create the defect does not allow for a precise depth of the osteochondral defect to be created which may have contributed to micro motion, hence fibrous tissue encapsulation, at the implant-bone interface.

In summary, a novel macroporous PVA hydrogel remained well fixed in an in vivo osteochondral defect. The implant performed favorably at all time-points and in all groups; it remained well fixed, did not cause inflammation or synovitis, and did not cause extensive damage to the opposing articular cartilage. Our hypothesis that matrix generation within the implant would be enhanced with collagenase predigestion was rejected, as similar results were achieved in the control group. Future studies are needed to improve integration of this porous hydrogel with bone, and to avoid the formation of a fibrous-tissue at the implant-tissue interface.

## Acknowledgments

We acknowledge funding provided by NIH (AR046121 & C06-RR12538-01), the Technology Development Funds at Hospital for Special Surgery, The Clark Foundation, and The Kirby Foundation. We thank Dr. Steven Arnoczky for his advice on the animal model and defect location; Dr. Peter Torzilli for his helpful comments, and Dr. Moira McCarthy for assistance during the rabbit surgeries.

## References

1. Shelbourne KD, Jari S, Gray T. Outcome of untreated traumatic articular cartilage defects of the knee: a natural history study. *J Bone Joint Surg Am.* 2003; 85(2):8–16. [PubMed: 12721340]
2. Buckwalter J, Mankin H. Articular cartilage: degeneration and osteoarthritis, repair, regeneration, and transplantation. *Instr Course Lect.* 1998; 47:487–504. [PubMed: 9571450]
3. Cole BJ, Lee SJ. Complex knee reconstruction: articular cartilage treatment options. *Arthroscopy.* 2003; 19(1):1–10. [PubMed: 14673413]
4. Bekkers JEJ, Inklaar M, Saris DIBF. Treatment selection in articular cartilage lesions of the knee. *Am J Sp Med.* 2009; 37(1):148S–55S.
5. Magnussen R, Dunn W, Carey J, Spindler K. Treatment of focal articular cartilage defects in the knee. *Clin Orthop Relat Res.* 2008; 466(4):952–62. [PubMed: 18196358]
6. Swieszkowski W, Ku D, Bersee H, Kurzydowski K. An elastic material for cartilage replacement in an arthritic shoulder joint. *Biomaterials.* 2006; 27(8):1534–41. [PubMed: 16188311]
7. Kobayashi M, Suong Hyu H. Development and evaluation of polyvinyl alcohol-hydrogels as an artificial articular cartilage for orthopedic implants. *Materials.* 2010; 3(4):2753–71.
8. Maher S, Doty S, Torzilli P, Thornton S, Lowman A, Thomas J, Warren R, Wright T, Myers E. Nondegradable hydrogels for the treatment of focal cartilage defects. *J Biomed Mater Res A.* 2007; 83(1):145–55. [PubMed: 17390320]
9. Ng K, Torzilli P, Warren R, Maher S. Biomechanical characterization of a macroporous polyvinyl alcohol scaffold for the repair of focal articular cartilage defects. *J Tissue Eng Regen Med.* 2012.1002/term.1510
10. Ng KW, Wanivenhaus F, Chen T, Hsu HC, Allon AA, Abrams VD, Torzilli PA, Warren RF, Maher SA. A novel macroporous polyvinyl alcohol scaffold promotes chondrocyte migration and interface formation in an in vitro cartilage defect model. *Tissue Eng Part A.* 2012; 18(11–12): 1273–81. [PubMed: 22435602]
11. Kleemann RU, Krockner D, Cedraro A, Tuischer J, Duda GN. Altered cartilage mechanics and histology in knee osteoarthritis: relation to clinical assessment (ICRS grade). *Osteoarthr Cartil.* 2005; 13(11):958–63. [PubMed: 16139530]
12. van den Borne MP, Raijmakers NJ, Vanlauwe J, Victor J, de Jong SN, Bellemans J, Saris DB. International Cartilage Repair Society (ICRS) and Oswestry macroscopic cartilage evaluation scores validated for use in autologous chondrocyte implantation (ACI) and microfracture. *Osteoarthr Cartil.* 2007; 15(12):1397–402. [PubMed: 17604187]



13. O'Driscoll SW, Keeley FW, Salter RB. The chondrogenic potential of free autogenous periosteal grafts for biological resurfacing of major full-thickness defects in joint surfaces under the influence of continuous passive motion. An experimental investigation in the rabbit. *J Bone Joint Surg Am.* 1986; 68(7):1017–35. [PubMed: 3745239]
14. Mak A, Lai W, Mow V. Biphasic indentation of articular cartilage—I. Theoretical analysis. *J Biomech.* 1987; 20(7):703–14. [PubMed: 3654668]
15. Oka M, Chang Y, Nakamura T, Ushio K, Toguchida J, Gu H. Synthetic osteochondral replacement of the femoral articular surface. *J Bone Joint Surg Br.* 1997; 79(6):1003–7. [PubMed: 9393921]
16. Noguchi T, Yamamuro T, Oka M, Kumar P, Kotoura Y, Hyon S, Ikada Y. Poly(vinyl alcohol) hydrogel as an artificial articular cartilage: evaluation of biocompatibility. *J Appl Biomater.* 1991; 2(2):101–7. [PubMed: 10171121]
17. Lee M, Sung K, Kurtis M, Akeson W, RLS. Adhesive force of chondrocytes to cartilage. Effects of chondroitinase ABC. *Clin Orthop Relat Res.* 2000; 370:286–94. [PubMed: 10660724]
18. van de Breevaart Bravenboer J, In der Maur C, Bos P, Feenstra L, Verhaar J, Weinans H, van Osch G. Improved cartilage integration and interfacial strength after enzymatic treatment in a cartilage transplantation model. *Arthritis Res Ther.* 2004; 6(5):R469–76. [PubMed: 15380046]
19. Hunziker E, Kapfinger E. Removal of proteoglycans from the surface of defects in articular cartilage transiently enhances coverage by repair cells. *J Bone Joint Surg Br.* 1998; 80(1):144–50. [PubMed: 9460972]
20. Mizuta H, Kudo S, Nakamura E, Takagi K, Hiraki Y. Expression of the PTH/PTHrP receptor in chondrogenic cells during the repair of full-thickness defects of articular cartilage. *Osteoarthr Cartil.* 2006; 14(9):944–52. [PubMed: 16644246]
21. Kienapfel H, Sprey C, Wilke A, Griss P. Implant fixation by bone ingrowth. *J Arthroplast.* 1999; 14(3):355–68.
22. Lambert E, Galante J, Rostoker W. Fixation of skeletal replacement by fiber metal composites. *Clin Orthop.* 1972; 87:303–10. [PubMed: 5078041]
23. Aspenberg P, Goodman S, Toksvig-Larsen S, Ryd L, Albrektsson T. Intermittent micromotion inhibits bone ingrowth. Titanium implants in rabbits. *Acta Orthop Scand.* 1992; 63(2):141–5. [PubMed: 1590046]
24. Lien S, Ko L, Huang T. Effect of pore size on ECM secretion and cell growth in gelatin scaffold for articular cartilage tissue engineering. *Acta Biomater.* 2009; 5(2):670–9. [PubMed: 18951858]
25. Raghunath J, Rollo J, Sales K, Butler P, Seifalian A. Biomaterials and scaffold design: key to tissue-engineering cartilage. *Biotechnol Appl Biochem.* 2007; 46:73–84. [PubMed: 17227284]
26. Melton J, Wilson A, Chapman-Sheath P, Cossey A. TruFit CB bone plug: chondral repair, scaffold design, surgical technique and early experiences. *Expert Rev Med Devices.* 2010; 7(3):333–41. [PubMed: 20420556]
27. Williams R, Gamradt S. Articular cartilage repair using a resorbable matrix scaffold. *Instr Course Lect.* 2008; 57:563–71. [PubMed: 18399610]
28. Maher, S.; Chen, D.; Deng, X.; Bradica, G.; Saska, R.; Castiglione, E.; Kronengold, R.; Torzilli, P. Paper No. 56—biomechanical evaluation of a biphasic scaffold for the repair of osteochondral defects by ex vivo indentation testing. New Orleans. Annual Meeting of the Orthopaedic Research Society; 2010.
29. Ushio K, Oka M, Hyon S, Yura S, Toguchida J, Nakamura T. Partial hemiarthroplasty for the treatment of osteonecrosis of the femoral head. An experimental study in the dog. *J Bone Joint Surg Br.* 2003; 85(6):922–30. [PubMed: 12931820]
30. Frisbie D, Oxford J, Southwood L, Trotter G, Rodkey W, Steadman J, Goodnight J, McIlwraith C. Early events in cartilage repair after subchondral bone microfracture. *Clin Orthop Relat Res.* 2003; 407:215–27. [PubMed: 12567150]

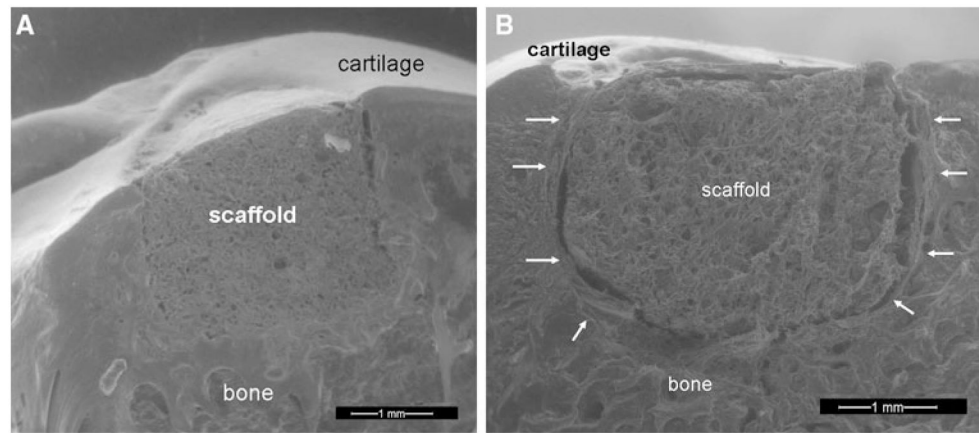


**Fig. 1.**

**a** Environmental scanning electron microscopy of a longitudinal slice taken through the cartilage-bone-implant. The specimen was retrieved at the 1 month post-operative time point. Good integration between the implant and the surrounding bone and articular cartilage was observed. **b** Environmental scanning electron microscopy image of a longitudinal slice taken through the cartilage-bone-implant construct at 3 months. Fibrous encapsulation of the implant is highlighted by *arrows*

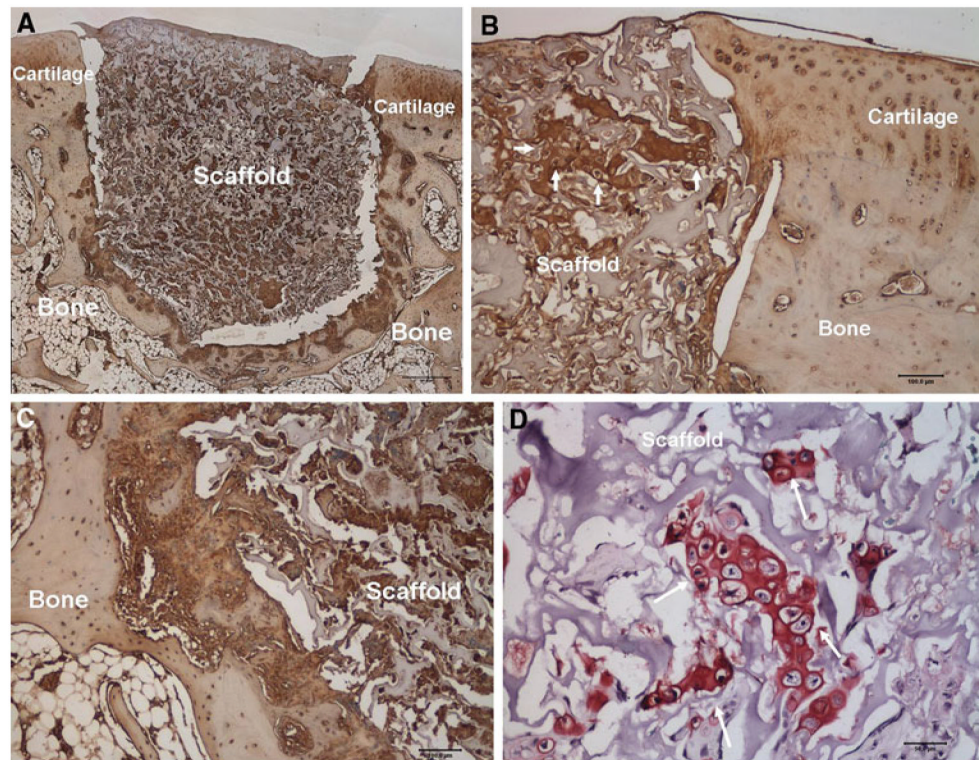


**Fig. 2.**  
**a** Aggrecan staining at 1 month demonstrates no degeneration of the articular cartilage adjacent to the implant ( $\times 1$ , *scale bar* represents 500  $\mu\text{m}$ ). **b** Aggrecan staining at 1 month demonstrates good integration of the implant with the adjacent articular cartilage ( $\times 10$ , *scale bar* represents 100  $\mu\text{m}$ , *arrows* point to clusters of chondrocyte-like cells producing aggrecan matrix). **c** Aggrecan staining at 1 month shows partial integration of the implant with adjacent bone, see *arrows* ( $\times 10$ , *scale bar* represents 100) within the implant producing proteoglycan ( $\times 40$ , *scale bar* represents 50  $\mu\text{m}$ ). **d** Safranin-O staining at 1 month demonstrates cells with chondrocyte-like morphology within the implant producing proteoglycan ( $\times 40$ , *scale bar* represents 50  $\mu\text{m}$ , *arrows* points to chondrocyte-like cells)

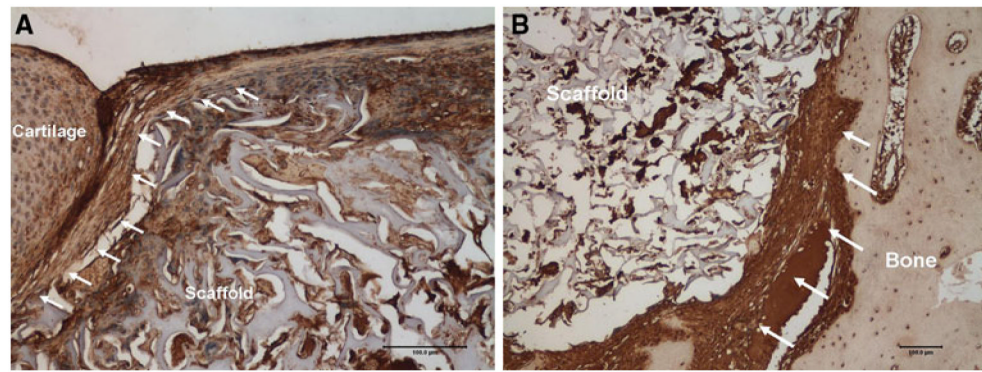


**Fig. 3.**

**a** Collagen type-I staining at 3 months demonstrates fibrous encapsulation of the implant with the adjacent articular cartilage ( $\times 10$ , *scale bar* represents 100  $\mu\text{m}$ , *arrows* point to encapsulating fibrous-tissue). **b** Collagen type-I staining at 3 months demonstrates fibrous encapsulation of the implant with the adjacent bony interface ( $\times 10$ , *scale bar* represents 100  $\mu\text{m}$ , *arrows* point to area of fibrous encapsulation between bone and implant)

**Table 1**

ICRS scores for collagenase and saline treated knees at the 1 and 3-month postoperative time-points

	<b>Defect repair</b>	<b>Integration</b>	<b>Macroscopic appearance</b>	<b>Overall ICRS score</b>
	<b>Max score: 4</b>	<b>Max score: 4</b>	<b>Max score: 4</b>	<b>Max score: 12</b>
1 month				
Collagenase (#10L)	3	3	4	10
Collagenase (#1R)	3	3	4	10
Collagenase (#2L)	3	4	4	11
Collagenase (#3R)	4	4	4	12
Collagenase (#6L)	3	4	4	11
Collagenase (#7R)	3	3	4	10
Saline (#10R)	3	4	4	11
Saline (#1L)	3	3	4	10
Saline (#2R)	3	3	4	10
Saline (#3L)	4	4	4	12
Saline (#6R)	3	4	4	11
Saline (#7L)	3	3	4	10
3 months				
Collagenase (#11L)	3	3	4	10
Collagenase (#12L)	4	4	4	12
Collagenase (#13R)	4	4	4	12
Collagenase(#14R)	3	4	4	11
Collagenase (#9R)	4	4	4	12
Saline (#11R)	4	3	4	11
Saline (#12R)	3	4	4	11
Saline (#13L)	4	3	3	10
Saline (#14L)	4	4	4	12
Saline (#9L)	3	4	4	11



**Table 2**

A summary of the histologic findings from collagenase treated and saline treated defects at the 1 and 3-month post-operative timepoints

Timepoint/group	Implant position	Damage to articular cartilage margins?	Implant-cartilage integration	Implant bone-integration	Chondrocyte-like cells present?
1 month ( <i>n</i> = 12 knees)					
Collagenase-treated ( <i>n</i> = 6)	<i>n</i> = 6 flush (100 %)	<i>n</i> = 6 none (100 %)	<i>n</i> = 6 integrated (100 %)	<i>n</i> = 3 partial integration (50 %) <i>n</i> = 3 fibrous integration (50 %)	<i>n</i> = 6 cells present (100 %)
Saline treated ( <i>n</i> = 6)	<i>n</i> = 6 flush (100 %)	<i>n</i> = 6 none (100 %)	<i>n</i> = 6 integrated (100 %)	<i>n</i> = 3 partial integration (50 %) <i>n</i> = 3 fibrous integration (50 %)	<i>n</i> = 6 cells present (100 %)
3 months ( <i>n</i> = 10 knees)					
Collagenase-treated ( <i>n</i> = 5)	<i>n</i> = 3 slightly recessed (60 %) 2 flush (40 %)	<i>n</i> = 6 none (100 %)	<i>n</i> = 6 fibrous integration (100 %)	<i>n</i> = 6 fibrous integration (100 %)	<i>n</i> = 2 cells present (40 %) <i>n</i> = 3 no cells (60 %)
Saline treated ( <i>n</i> = 5)	<i>n</i> = 2 slightly recessed (40 %) <i>n</i> = 3 flush (60 %)	<i>n</i> = 6 none (100 %)	<i>n</i> = 6 fibrous integration (100 %)	<i>n</i> = 6 fibrous integration (100 %)	<i>n</i> = 3 cells present (60 %) <i>n</i> = 2 no cells (40 %)

The following was assessed: whether or not the implant surface was recessed relative to the surface of the articular cartilage (implant position); whether or not there was damage to articular cartilage at the periphery of the implant; whether or not fibrous-tissue was interposed between the implant and adjacent bone (implant-cartilage integration); and whether or not chondrocyte-like cells were present within the pores of the implant

**Table 3**

Area quantification of aggrecan staining adjusted for scaffold porosity

<b>Timepoint</b>	<b>Collagenase-treated (% <math>\pm</math> SD)</b>	<b>Saline control (% <math>\pm</math> SD)</b>
1 month ( $n = 12$ )	16.6 ( $\pm 0.76$ )	12.5 ( $\pm 4.6$ )
3 months ( $n = 10$ )	14.5 ( $\pm 6.7$ )	10.7 ( $\pm 0.59$ )